JOURNAL OF CATALYSIS **163,** 195–203 (1996)
ARTICLE NO. 0319

Iron-Based Dehydrogenation Catalysts Supported on Zirconia

II. The Behavior in the Dehydrogenation of 1-Butene

L. A. Boot,*,[1] A. J. van Dillen,* J. W. Geus,* and F. R. van Buren†

*Department of Inorganic Chemistry, Debye Institute, Utrecht University, P.O. Box 80083, 3508 TB Utrecht, The Netherlands; and †Dow Benelux N.V., P.O. Box 48, 4530 AA Terneuzen, The Netherlands

Received August 15, 1995; revised June 7, 1996; accepted June 12, 1996

The behavior of iron oxide-based catalysts supported on zirconia in the dehydrogenation of 1-butene was investigated. Iron oxide-on-zirconia catalysts deactivate during operation due to carbon deposition. It was shown with XRD that solid state reactions between the active phase and the support do not take place in the zirconia-supported catalysts: the iron-containing phase after reaction is Fe_3O_4. The total amount of carbon deposited onto zirconia-supported catalysts containing only iron oxide as determined with temperature-programmed oxidation is about 2 wt% C after 20 h. It was also shown that a carbon species deposited in narrow pores was present in iron oxide-on-zirconia catalysts. The KFe/ZrO_2 catalysts proved to be more stable than KFe/MgO catalysts: for catalysts containing highly dispersed iron oxide only a slight deactivation was observed after about 100 h on stream. This deactivation is attributed to migration of potassium from the catalyst to the quartz reactor. Catalysts of low loadings (1 wt% Fe, 1 wt% K) or with less well-dispersed iron oxide deactivate in a shorter period of time: an incomplete coverage of the zirconia support leads to deactivation by carbon deposition. The selectivity to butadiene of the KFe/ZrO_2 catalysts is about 60%, which is related to a high production of CO_2. This is attributed to carbon deposition taking place in the small pores of the zirconia-supported catalysts. The coke is subsequently gasified, probably by the supported potassium carbonate. Eliminating the small pores substantially improved the butadiene selectivity.

1. INTRODUCTION

The use of a supported iron oxide catalyst can circumvent the mechanical degradation of the unsupported dehydrogenation catalysts due to the structural transformation of the iron oxide phase under reaction conditions (1). The concept of using an oxidic support in dehydrogenation catalysts has been reintroduced by Stobbe *et al.* Stobbe described in his thesis (2) and related papers (3–6) the preparation, characterization, and testing in the dehydrogenation of 1-butene of an iron oxide-based catalyst supported on preshaped magnesia support bodies. However, MgO is liable to reaction with water vapor and carbon dioxide from atmospheric air, which causes the formation of magnesium hydroxide and (hydroxy-)carbonates. Therefore, it can be suspected that the magnesia-supported catalyst is less stable during, e.g., storage or plant start-up. In the present work, an alternative support material is studied. In view of its properties which are described in the literature (7), zirconium dioxide (zirconia) is a candidate catalyst support material for application in dehydrogenation processes.

In a preceding paper, the preparation and characterization of zirconia-supported iron oxide-based catalysts were reported (1). It was demonstrated that a homogeneously distributed, well-dispersed iron oxide-on-zirconia catalyst could be prepared using incipient wetness impregnation of preshaped support bodies. Also the addition of potassium, the component required for keeping the active surface free from deactivating carbonaceous deposits, was investigated. In this paper the behavior of the obtained catalysts in the dehydrogenation of 1-butene is described. The results of the test reaction will establish whether the concept of using a supported iron oxide-based dehydrogenation catalyst can be extended to another support material, viz., zirconium dioxide.

The first and principal property that is dealt with is the deactivation behavior of the Fe/ZrO_2 and $Fe,K/ZrO_2$ catalysts. Subsequently the catalytic performance including the selectivity to butadiene is discussed. Also the deposition of carbon as a cause for deactivation is examined. Finally, from temperature-programmed activity measurements kinetic parameters for butene dehydrogenation over zirconia-supported Fe,K catalysts are determined.

2. METHODS

Catalyst Preparation

Catalysts were prepared according to procedures described previously (1). A short description will be given here.

[1] Present address: Akzo Nobel Chemicals B.V., P.O. Box 37650, 1030 BE Amsterdam, The Netherlands. E-mail: Ludo.Boot@Akzo.NL.

0021-9517/96 $18.00

Zirconia bodies were obtained from various manufacturers: Daiichi RSC-H, monoclinic ZrO_2 pellets, ϕ 3 mm (batches I and II (7)); Engelhard L6132 pellets (ca. 60% monoclinic – 40% tetragonal), ϕ 3 mm; and Norton XZ 16052, monoclinic ZrO_2 extrudates, ϕ 3 mm. Prior to impregnation, the supports were precalcined at 850°C in air for 16 h to obtain stable specific surface areas of about 20 m^2/g and pore volumes of 0.25, 0.17, and 0.22 ml/g, respectively.

The pretreated supports were impregnated to incipient wetness using either a solution of ammonium iron (III) citrate (Merck, 28% Fe) or a solution of both ammonium iron (III) citrate and potassium carbonate. In some cases catalysts were impregnated with iron (III) nitrate or ammonium iron (III) EDTA to be able to investigate the influence of the iron precursor on the iron oxide distribution and on the catalytic performance. After drying at room temperature, the catalysts were calcined in air at 750°C for 16 h.

Catalyst Characterization

X-ray diffraction. Powder XRD was carried out with Fe$K\alpha_{1,2}$ radiation (1.93735 Å) in a Philips powder diffractometer mounted on a Philips PW1140 X-ray generator.

Temperature-programmed oxidation. Determination of the amount of deposited carbon was performed immediately after the test reaction by TPO using 5 v% O_2 in N_2 (50 ml/min). Fractured catalyst samples (0.150–0.425 mm) were oxidized using a heating rate of 3°C/min. Carbon was detected as CO_2 in a gas chromatograph (Porapak Q column, 1/8″, 2.5 m; He carrier gas; 160°C) equipped with a thermal conductivity detector. Using a mass spectrometer it was verified that the production of CO during TPO was negligible.

Catalyst Testing

Nonoxidative butene dehydrogenation was carried out in a semiautomated flow apparatus, as schematically represented in Fig. 1. A detailed description of the different components is given in Stobbe's thesis (2). The main difference is the location of the temperature measurement and control. A thermocouple inserted in a small, sealed quartz tubing (ϕ 3 mm) was inserted through the top of the quartz reactor to measure the temperature inside the catalyst bed, downstream with respect to the gas flow.

A gas mixture (atmospheric pressure) of 5v% 1-butene (Hoek Loos, 2.5), 30v% steam (added by passing the gas flow through a saturator kept at 70°C) in N_2 (Hoek Loos, 5.0), resulting in a water/1-butene ratio (mole/mole) of 6, was passed upflow through the catalyst bed which had previously been heated up in air to 600°C. Temperature-programmed activity measurements were performed in the temperature range of 425–625°C, using a water/1-butene ratio of 8.3. About 1 g of catalyst (sieve fraction, 0.50–0.85 mm) was used at a gas flow rate of 50 ml/min,

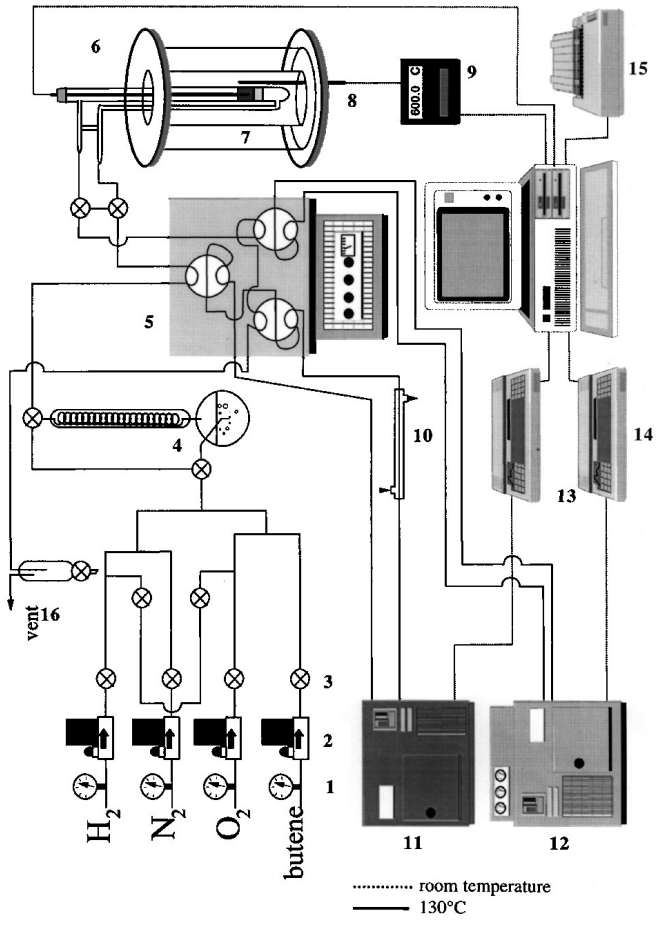

FIG. 1. Schematic representation of the flow apparatus used for butene dehydrogenation (7).

resulting in a weight hourly space velocity (WHSV) of 0.35 $g_{butene}/(g_{catalyst} \cdot h)$. By using the same catalyst mass in all tests, the WHSV was kept constant when testing catalysts based on the various support oxides which have different specific densities. To investigate the activity of a carbon surface the catalytic performance of an activated carbon sample (Printex U, 110 m^2/g) was tested.

Calculations of the conversion, the selectivity to product *i*, and the yield of product *i* were carried out in the same manner as was done earlier (2, 4, 6),

$$\text{Conversion (\%)} = \frac{\sum n(i) \cdot \text{Prod.}(i)}{\sum n(i) \cdot \text{Prod.}(i) + \text{Butenes (after)}} \cdot 100\% \quad [1]$$

$$\text{Selectivity } i\,(\%) = \frac{n(i) \cdot \text{Prod.}(i)}{\sum n(i) \cdot \text{Prod.}(i)} \cdot 100\% \quad [2]$$

$$\text{Yield } i\,(\%) = \frac{n(i) \cdot \text{Prod.}(i)}{\sum n(i) \cdot \text{Prod.}(i) + \text{Butenes (after)}} \cdot 100\%, \quad [3]$$

where Prod. (i) refers to the concentration of product i in mole/l; $n(i)$ refers to the ratio between the number of carbon atoms in product i and the number of carbon atoms in butene; Butenes (after) is the total amount of unreacted butenes. The denominator in Eqs. [1] and [3] thus equals the concentration of butenes in the feed. The linear butene isomers are all considered as reactants, since the dehydrogenation of these compounds proceeds similarly (4).

3. RESULTS AND DISCUSSION

Iron Oxide-on-Zirconia Catalysts

Butene conversions and selectivities to butadiene as a function of time at 600°C for iron oxide-on-zirconia catalysts containing different amounts of iron are presented in Figs. 2a and 2b, respectively. The byproduct yields for a 3 wt% Fe/ZrO_2 catalyst are shown in Fig. 3. The butene conversion and butadiene selectivity for the bare support material are presented in Fig. 4.

As can be seen in Fig. 2a Fe/ZrO_2 catalysts deactivate at 600°C during the reaction. For a catalyst containing 3 wt% Fe the butene conversion has decreased from an initial value of about 45% to a level of about 13% after approximately 4.5–5 h. The latter conversion level is observed for all catalysts after the deactivation has completed (also for catalysts containing magnesia or titania as the support (4, 7)), for the bare support material (Fig. 4), and for a sample of activated carbon (Printex U; not shown). It seems to be characteristic for an inert catalyst surface which is covered by carbonaceous deposits. It can be calculated from thermodynamics (4, 8, 9) that carbon deposition will take place under the conditions used in these experiments.

Two processes that take place upon the exposure of the catalysts to the feed, viz., *carbon deposition* and *reduction* of the supported iron oxide phase, both influence the deactivation behavior. With X-ray diffraction Fe_3O_4 is shown to be present in the Fe/ZrO_2 catalysts after the catalytic reaction. Reduction of Fe_2O_3 to Fe_3O_4 increases the selectivity toward butadiene and the butadiene yield,since Fe_3O_4 is

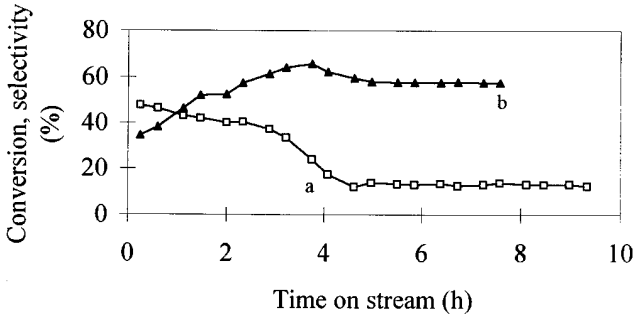

FIG. 2. 1-Butene conversion (a) and 1,3-butadiene selectivity (b) versus time-on-stream for a zirconia-supported 3 wt% Fe catalyst (ex citrate, on Daiichi (I) support, 600°C).

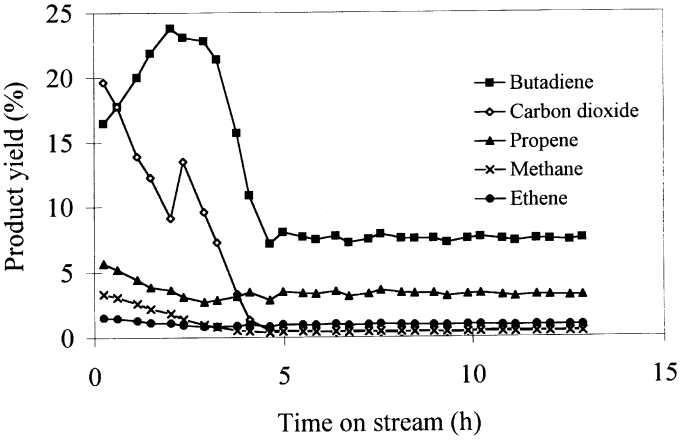

FIG. 3. Product yield plots for the various products versus time-on-stream for a 3 wt% Fe/ZrO_2 catalyst (ex citrate, on Daiichi (I) support, 600°C).

the more selective phase in dehydrogenation (10). Stated alternatively, α-Fe_2O_3 behaves as a catalyst for deep oxidation and produces CO_2. The reduction of α-Fe_2O_3 and production of CO_2 initially compensate the loss in butene conversion due to carbon deposition. When the reduction is complete, a higher rate of deactivation, due to carbon deposition only, is observed. The course of the decreasing conversion observed with the 3 wt% Fe/ZrO_2 catalyst (Fig. 2a) can indeed be divided into two regions, the first showing a low deactivation rate and the second showing a rapid deactivation. This would indicate that the deactivation is governed by the above two effects, which operate successively as described.

However, carbon deposition alone could also be responsible for the observed deactivation process. The plot can also be fitted by a sigmoidal carbon deposition model, e.g., as proposed by Dadyburjor *et al.* (11), which is characterized by an autocatalytic initiation/propagation mechanism of coke deposition. Therefore, more information

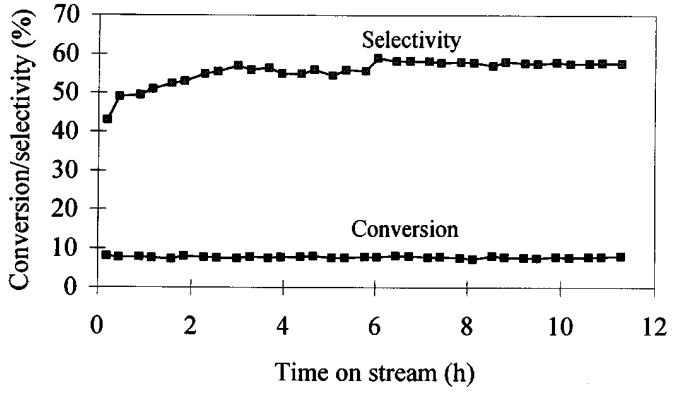

FIG. 4. 1-Butene conversion and selectivity versus time-on-stream for the bare zirconia support (Daiichi (I), 600°C).

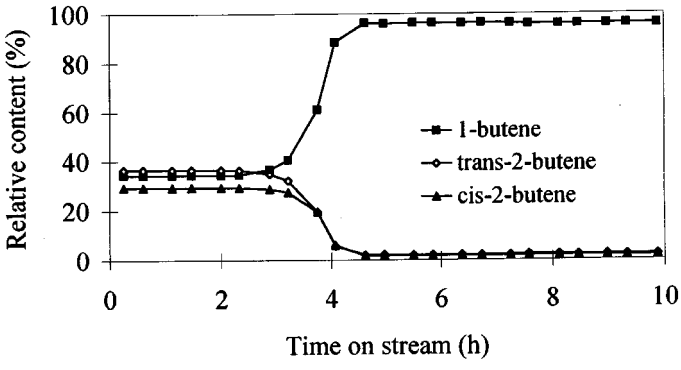

FIG. 5. Relative distribution of butene isomers versus time-on-stream for a 3 wt% Fe/ZrO_2 catalyst (ex citrate, on Daiichi (I) support, 600°C).

(deactivation behavior of other catalysts and the product selectivity plots) has to be studied to discriminate between the two models.

The type of catalyst support did not influence the catalytic properties of the Fe/ZrO_2 system. The iron loading seems to affect the time required to complete the deactivation, but does not have a large effect on the overall catalytic behavior.

In Fig. 2b it can be seen that the initial selectivity towards butadiene formation is low, about 35 to 50%. From the product yield plot (Fig. 3), it can be deduced that this low selectivity is caused by an oxidation of part of the hydrocarbons to carbon dioxide by oxygen originating from the applied iron oxide which is being reduced by the hydrocarbons. The selectivity passes through a maximum before assuming a constant level. The CO_2 production, and, hence, the iron oxide reduction, stops at the same point in time as the deactivation has completed. The butadiene selectivity maximum coincides with a slight minimum in the propene yield and not with the expected completion of the reduction to Fe_3O_4, the phase which shows the highest selectivity towards butadiene (10).

More information can be obtained from the isomerization reaction taking place. Figure 5 shows that the isomerization reaction of 1-butene to its isomers *cis*- and *trans*-2-butene proceeds rapidly until the start of the period of rapid deactivation is reached. This is an indication that from that moment on the surface becomes covered with carbonaceous deposits, since all deactivated catalysts (also catalysts containing other supports) as well as the activated carbon sample show a low activity in the isomerization reaction. This low activity can probably be attributed to a decreased adsorption of 1-butene on the deactivated catalyst surface.

The information discussed above brings us to the following explanation for the observed deactivation behavior. In the first stage of the deactivation hardly any carbon deposition occurs on the iron oxide surface, due to immediate oxidation of the deposits by the active component. Adsorbed butene molecules either are oxidized completely or desorb as butene isomer or as butadiene. As the reduction of the catalyst proceeds, the fraction of Fe_3O_4 increases, the deep oxidation activity decreases, and the butadiene yield increases. Just before completion of the reduction process, the oxidation reaction can no longer keep up with the carbon deposition, and a rapid covering of the active surface with carbon occurs. This is evidenced by the drop of the conversion and the sudden disappearance of the isomerization activity.

As compared with the magnesia-supported catalysts reported on earlier by Stobbe *et al.* (4), a different behavior is observed for the iron-on-zirconia system. The iron-on-magnesia catalysts deactivate more slowly after an initial activation which was explained by reduction of the supported iron oxide phase. Product yield plots explain this phenomenon: the carbon dioxide production continues until about 10 h after the start of the catalytic reaction. Consequently, the coverage of the active surface proceeds more gradually. The observed by-product selectivities do not show large differences for both catalyst systems.

Effect of Addition of Potassium

To determine the stability of the catalytic performance of the zirconia-supported catalysts containing both iron and potassium, butene conversion and butadiene selectivity was monitored at 600°C as a function of time-on-stream. These variables are shown for iron oxide catalysts with various loadings of both components in Figs. 6 and 7. The yield of the various products is plotted in Fig. 8.

It can be seen in Fig. 6 that there is no clear correlation between the iron and potassium loadings and the conversion of butene and the selectivity to butadiene. Figure 6

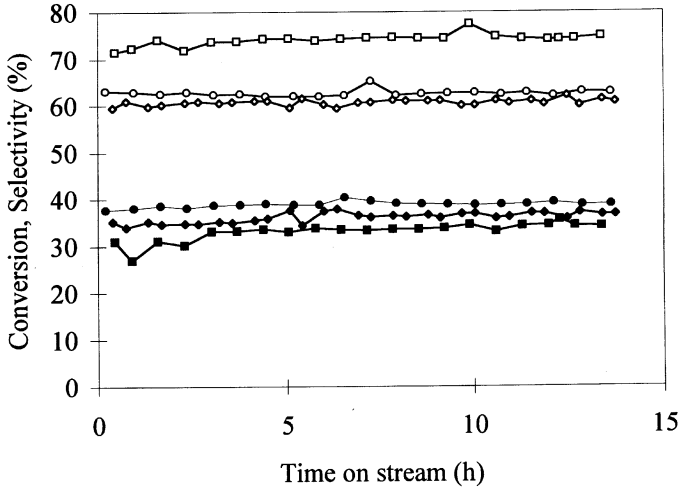

FIG. 6. 1-Butene conversion and 1,3-butadiene selectivity versus time-on-stream for zirconia-supported catalysts with various iron and potassium loadings (600°C, ex citrate, and potassium carbonate, on Daiichi (I) support, 600°C). Filled symbols, conversion; open symbols, selectivity: ●, 3–3 wt% Fe-K; ◆, 3–9 wt% Fe-K; ■, 9–9 wt% Fe-K.

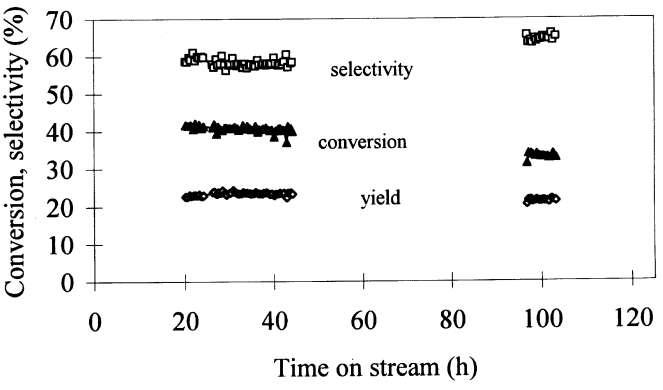

FIG. 7. Prolonged test of the 1-butene conversion and 1,3-butadiene selectivity versus time-on-stream for a 6 wt% Fe, 9% K/ZrO_2 catalyst (ex citrate, and potassium carbonate, on Daiichi (I) support, 600°C).

shows a higher selectivity to butadiene for the catalyst with 9 wt% Fe and 9 wt% K. However, in the complete (3×3) matrix of catalysts with varying loadings no correlation was found. If the iron or potassium loading is below 1 wt%, however, the catalysts deactivate. With a catalyst containing only 0.25 wt% Fe and 0.25 wt% K, for instance, a decrease in conversion is observed starting after about 2 h on stream.

This deactivation is attributed to carbon deposition, since the isomerization activity decreases parallel to the conversion as was also noted with the catalysts without potassium. This deactivation can also be observed with catalysts which show an inhomogeneous distribution of the iron/potassium phase after preparation. It therefore seems likely that the coverage of the support surface with the iron oxide-potassium oxide phase plays a crucial part in catalyst stability. Possibly the growth of carbon initiates on the bare surface of the zirconia support.

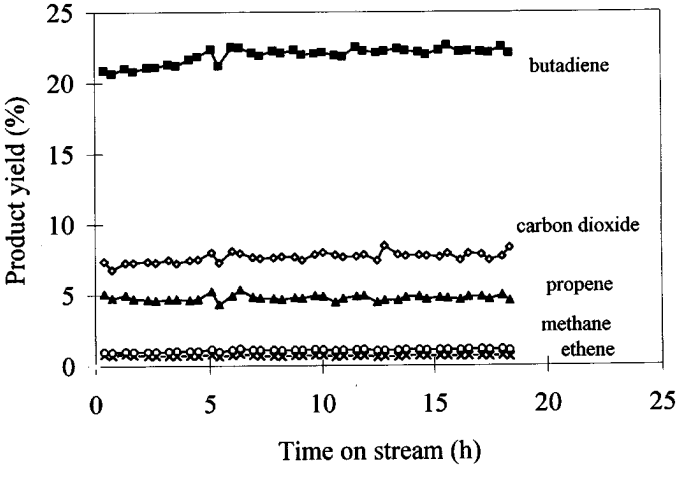

FIG. 8. Product yield plots for the various products versus time-on-stream for a 3 wt% Fe, 9% K/ZrO_2 catalyst (ex citrate, and potassium carbonate, on Daiichi (I) support, 600°C).

The results of the prolonged test presented in Fig. 7 show that with a catalyst containing 6% Fe and 9% K after about 100 h a small decrease of the conversion has occurred. Whether this is due to some intrinsic deactivation phenomenon or to potassium loss to the quartz reactor cannot be decided with certainty. Formation of potassium silicate in the reactor wall was observed with the potassium containing zirconia-supported catalysts. With the Fe,K/MgO catalysts described by Stobbe *et al.* (6), deactivation was observed for catalysts with similar Fe and K loadings already after 30 h on stream. No change in the isomerization activity, which would be indicative of carbon deposition, is observed with the zirconia-supported samples after 100 h. This leads to the conclusion that potassium depletion causes the deactivation observed after long times-on-stream.

A remarkable difference with the (Fe,K) catalysts supported on magnesia or with the reference bulk iron oxide-based catalyst S-105 (6) is the low selectivity toward the formation of 1,3-butadiene which is characteristic for the zirconia-supported catalysts. As can be seen in Fig. 8, the low selectivity is related to a high carbon dioxide production. The zirconia-supported catalysts produce carbon dioxide in large quantities, whereas other products, such as propene, show comparable yields.

To obtain more information on the deposition of carbon on the catalysts, temperature-programmed oxidation of various zirconia-supported catalysts immediately after performing the test reaction was carried out. Comparison with the data reported for magnesia-supported catalysts (4) should reveal whether the carbon deposition is more pronounced with zirconia as the support. Alternatively, a different active phase which possesses a higher activity for deep oxidation could be present in the $Fe,K/ZrO_2$ catalysts under reaction conditions. By determining the activation energies for the dehydrogenation reaction, information about the active phase present under reaction conditions is obtained. With XRD, the nature of the iron-containing phase in the $Fe,K/ZrO_2$ catalysts before (1) and after reaction could not be established. Finally, the carbon dioxide could result from direct oxidation of the hydrocarbons caused by diffusion limitations: the zirconia-supported samples contain narrower pores than the other two catalysts and the pore size has been shown to have a great influence on the selectivity in dehydrogenation reactions (10, 12). Performing catalytic measurements with smaller catalyst particles should give information on any diffusion limitations. The influence of the pore size distribution is evaluated by testing a catalyst which is prepared by impregnation of a zirconia-support which was sintered at 1100°C and therefore contains mainly larger pores (7).

Carbon Deposition

The temperature-programmed oxidation of carbon deposited on Fe/ZrO_2 and $Fe,K/ZrO_2$ catalysts are presented

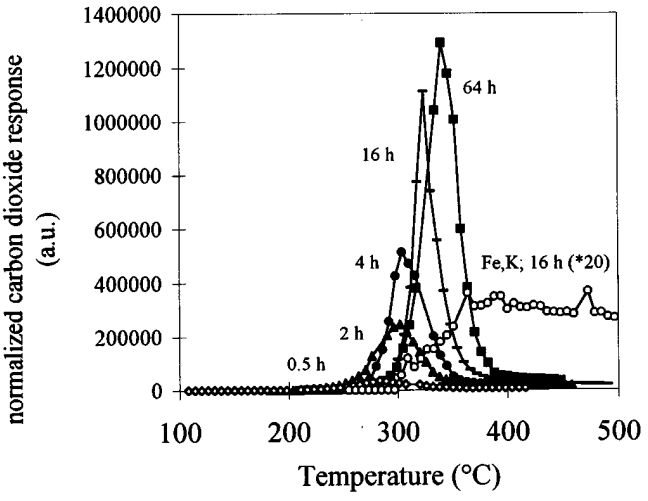

FIG. 9. Temperature-programmed oxidation profiles for a 3 wt% Fe/ZrO_2 and (3 wt% Fe, 3 wt% K)/ZrO_2 catalysts after various times-on-stream at standard butene dehydrogenation conditions (ex citrate and ex citrate and potassium carbonate, respectively, on Daiichi (II) support).

in Fig. 9. The total carbon deposition on a Fe/ZrO_2 catalyst as a function of time is plotted in Fig. 10.

For the iron oxide-on-zirconia catalyst a carbon deposition which increases steadily with time-on-stream is observed (Figs. 9 and 10). The oxidation of the deposited carbon seems to take place in one step. It must be remarked, however, that the CO_2 peak shows a small but long tail indicative of the formation of carbon which cannot be oxidized readily, e.g., carbon present in the micropores of the catalyst. This was checked by maintaining the temperature constant at 425°C, until CO_2 could no longer be detected with the chromatograph. When the temperature was raised again, no CO_2 was detected, which points to the transport limitation with the oxidation of these deposits. This badly accessible carbon is formed almost instantly, whereas the readily accessible carbon starts to build up after about 0.5–1 h. Apparently, the readily accessible carbon becomes more structurally organized with time: the onset temperature of oxidation shifts from about 250°C for carbonaceous deposits resulting after shorter deposition times to 280°C for coke oxidized after 16 h on stream.

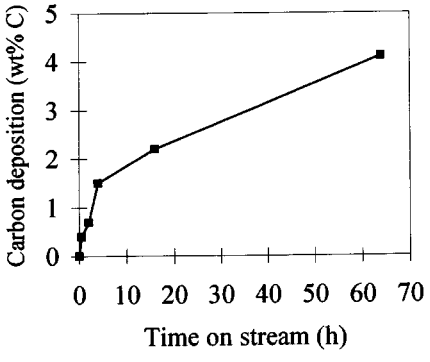

FIG. 10. Total carbon deposition versus time-on-stream at standard butene dehydrogenation conditions (600°C) as calculated from temperature-programmed oxidation profiles for a 3 wt% Fe/ZrO_2 catalyst (ex citrate. Daiichi (II) support).

In the total carbon deposition plot (Fig. 10), two rates of carbon deposition can be distinguished with the Fe/ZrO_2 catalysts. Initially, the deposition rate is high. After about 4 h coking proceeds at a lower rate. This period is about equal to the time required for a 3 wt% Fe/ZrO_2 catalyst to deactivate to a constant level (cf. Fig. 2a). Therefore, it can be assumed that the carbon deposits have covered the entire active surface at that stage. The low deposition rate is probably characteristic for deposition of carbon onto carbon. The decreased adsorption of the coke-forming reactants and products at the surface (cf. the isomerization activity, Fig. 5) are probably responsible for the lower rate of carbon deposition. Furthermore, based on the specific surface area of the catalyst (ca. 20 m^2/g(1)) and the density and interatomic distances of graphite, an average layer thickness of about one monolayer can be calculated for 1.5 wt% C deposited on the catalyst. This also corresponds with the deflection point in Fig. 10.

Catalysts containing also potassium show different coking properties than the Fe/ZrO_2 sample (Fig. 9). First, the amount of deposited carbon is about 15 to 20 times less after 16 h on stream. Second, catalysts with potassium seem to build up only the type of coke which was designated above as the "badly accessible" type. It is clear that in catalysts with potassium the carbon deposition is not prevented entirely. The detected CO_2 in the TPO experiments is not generated by the reaction of iron (III) oxide with potassium carbonate to $KFeO_2$ and CO_2, which may be expected to proceed in this temperature range (1, 7). This was checked by heating a fresh catalyst in nitrogen: any amount of CO_2 formed by the solid state reaction was too small to be detected.

Temperature-Programmed Measurements and Kinetic Parameters

Results of temperature-dependent measurements of butene conversion, butadiene selectivity and product yields for a $Fe,K/ZrO_2$ catalyst are shown in Figs. 11 and 12.

In Fig. 11 it can be seen that the onset temperature of butene conversion for the $Fe,K/ZrO_2$ catalyst in 450°C, which is about the same as that measured with Fe,K/MgO catalysts. Also the temperature at which a conversion of 40% is reached (T_{40}) is about equal for both catalysts, viz., 595°C. The selectivity to 1,3-butadiene at that temperature (S_{40}), however, is only 63% for the $Fe,K/ZrO_2$ catalyst, versus 83–84% for Fe,K/MgO catalysts. Figure 12 demonstrates that this is related to a higher production of CO_2. Furthermore, in Fig. 11 a step is present in the selectivity plot. This is caused by a related step in the CO_2 yield at

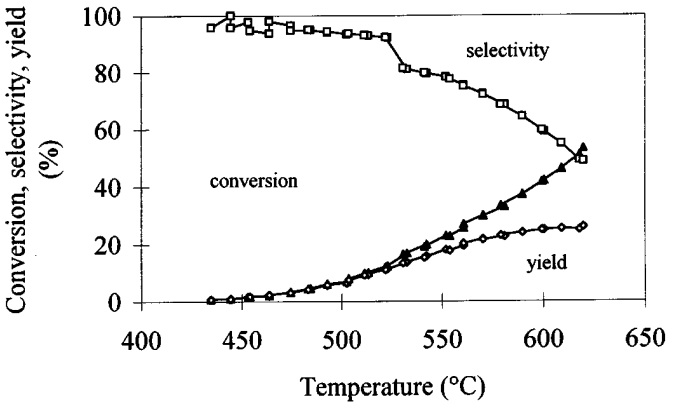

FIG. 11. 1-Butene conversion and 1,3-butadiene selectivity versus temperature for a 3 wt% Fe, 9% K/ZrO_2 catalyst (on Daiichi (I) support).

about 530°C. If the activity curve is measured at decreasing temperatures, a sudden stepwise end of the CO_2 formation is observed also. This may be attributed to the formation of the badly accessible carbon, which was encountered in TPO. Above about 530°C the carbon can be oxidized, whereas below these temperatures it is not removed by the gasification reaction.

From the temperature-dependent activity plots Arrhenius plots have been constructed and apparent activation energies for the dehydrogenation reaction have been calculated following the procedure described by Stobbe *et al.* (4, 6). The obtained values are listed in Table 1. All kinetic data have been derived from 1-butene conversions below 10%.

In Table 1 it can be seen that there is a scattering in the calculated activation energies of 6 kJ/mole above and below the average value of about 149 kJ/mole. If this experimental uncertainty is taken into account, the apparent activation energies shown by the Fe,K/ZrO_2 catalysts are somewhat lower than the values of about 155 kJ/mole reported by

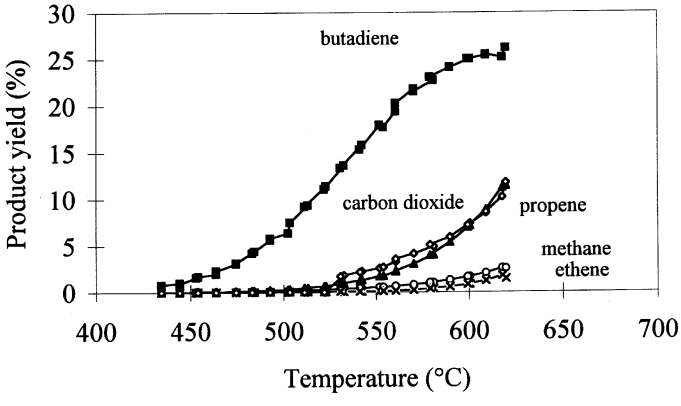

FIG. 12. Product yield plots for the various products versus temperature for a 3 wt% Fe, 9% K/ZrO_2 catalyst (on Daiichi (I) support).

TABLE 1

Kinetic Parameters and Performance Data for (Fe,K)/ZrO_2 Catalysts

Catalyst loading		E_a	ln k_0	T_{40}	S_{40}
Fe (wt%)	K (wt%)	(kJ/mole)	(ln [atm/(min · g cat)])[a]	(°C)	(%)
1	1	147	21.5	[b]	[b]
3	3	150	22.1	599	62
3	6	155	24.1	599	60
3	9	144	19.7	605	63
3	30	148	19.9	619	70
9	3	143	19.2	590	62
9	9	147	19.9	608	63

Note. E_a, activation energy; ln k_0, ln pre-exponential factor; T_{40}, temperature at which 40% conversion is reached; S_{40}, selectivity to 1,3-butadiene at 40% conversion.

[a] ln k_0 has been calculated with $E_a = 149$ kJ/mole.

[b] Deactivates at higher temperatures before reaching 40% conversion.

Stobbe *et al.* (6) for Fe,K/MgO catalysts. The temperatures T_{40} are slightly higher than most temperatures reported by Stobbe *et al.* (about 590°C), but are equal to the T_{40} values reported for the S-105 reference catalyst and the Fe,K/MgO catalyst which was exposed to atmospheric air. Since the Fe,K/ZrO_2 catalysts have also been exposed to air before determining the catalytic activity, the values of T_{40} agree. It seems that there is an influence of the potassium loading. At equal iron loading an increased potassium loading results in a higher T_{40}. This might be due to a decrease of the accessible active surface area. The selectivity at 40% conversion (S_{40}) is lower for all zirconia-supported catalysts, as was discussed previously.

Transport Limitations

Calculations performed to determine the Thiele modulus Φ_s and effectiveness factor η did not indicate that diffusion limitations are present: η was estimated to be equal to unity for the zirconia-supported catalysts (13). Performing catalytic measurements with smaller catalyst particles should give experimental evidence to confirm whether transport limitation is indeed absent (12), but no effect of the used catalyst sieve fraction on the performance was observed. However, diffusion limitations were observed with the temperature-programmed oxidation of the carbonaceous deposits. The presence of narrow pores may affect the coking and gasification properties of the catalysts. This was checked by testing a catalyst which was prepared using a support material which was precalcined at a substantially higher temperature, viz., 1100°C, prior to impregnation. This procedure eliminates the smaller pores to a great extent (7). The calculated micropore surface is reduced to about 0.8 m^2/g, as opposed to about 3 m^2/g for a support treated at 850°C. The butene conversion and butadiene selectivity of this catalyst are plotted in Fig. 13.

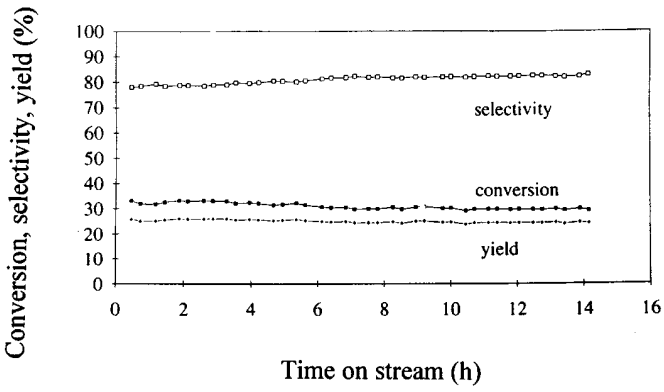

FIG. 13. 1-Butene conversion, 1,3-butadiene selectivity, and butadiene yield versus time-on-stream for a zirconia-supported catalyst prepared with a support precalcined at 1100°C (1 wt% Fe, 1 wt% K, on Daiichi (II) support, 600°C).

It can be seen in Fig. 13 that the 1,3-butadiene selectivity is about 80% for the catalyst on the sintered support. Simultaneously, the activity at 600°C has decreased to about 30%. This indicates that the texture of the zirconia support plays a role in the observed selectivity behavior. If a high butadiene selectivity is needed at equal butadiene yields, the use of a sintered support is a way to meet with this requirement.

4. FURTHER DISCUSSION AND CONCLUSIONS

The iron oxide-on-zirconia catalysts deactivate during operation due to carbon deposition within about 4 h. This period is intermediate between magnesia- and titania-supported catalysts (4, 7). The explanation for this order can be found in the deactivation mechanism.

In titania-supported catalysts the formation of $FeTiO_3$ occurs very rapidly, which deactivates the catalyst (7, 14). It was shown with XRD that bulk solid state reactions between the active phase and the support do not take place in the zirconia-supported catalysts: the iron-containing phase after reaction is Fe_3O_4. Magnesia-supported catalysts deactivate due to carbon deposition (4), but at a slower rate than the zirconia-supported catalysts. Comparison with the values reported by Stobbe *et al.* (4) show that the total amount of carbon deposition onto zirconia-supported catalysts containing only iron oxide as determined with TPO is about equal to that found with magnesia-supported catalysts. However, it was also shown that a carbon species deposited in narrow pores was present in Fe/ZrO_2 samples. The different deactivation behavior can therefore be understood from the location of the deposited coke.

Coke is deposited instantly in the narrow pores. Simultaneously, the active phase is reduced from α-Fe_2O_3 to Fe_3O_4, which increases the selectivity toward butadiene. The butadiene yield increases also, since the rise in the selectivity is higher than the decrease in the conversion due to a decreasing carbon dioxide production. At a certain point in time, the iron oxide reduction is complete and the coke layer growing from the deposits which were present from the beginning starts to cover the active phase. This lowers the butadiene yield immediately, and consequently, at constant by-product formation rates, also the butene conversion. The fact that coke is deposited instantly and is able to grow from the small pores to cover the entire catalyst surface explains the shorter period of time involved in the deactivation than that seen with the magnesia-supported catalysts. Nucleation of coke on the (basic and wide pore) magnesia support is likely to proceed more slowly and the deactivation therefore follows a less steep trajectory.

However, the $Fe,K/ZrO_2$ catalysts proved to be even more stable than the Fe,K/MgO catalysts: for well-dispersed catalysts only a slight deactivation was observed after about 100 h on stream. This deactivation is attributed to migration of potassium from the catalyst to the wall of the quartz reactor. Catalysts with very low loadings or less well-dispersed catalysts deactivate in a shorter period of time. This indicates that an incomplete coverage of the zirconia support leads to deactivation by carbon deposition.

The selectivity to butadiene of the $Fe,K/ZrO_2$ catalysts is relatively low, which is related to a high production of carbon dioxide. This is not attributed to a higher deep oxidation activity of these catalysts, nor to diffusion limitations favoring sequential oxidation of the butadiene. The origin of the high CO_2 production lies in the fact that carbon deposition is taking place in the narrow pores of the zirconia-supported catalysts. This coke is subsequently gasified, probably by the supported potassium carbonate when the deposited layer has grown to such an extent that it reaches the supported phase. Eliminating the small pores by sintering treatments at high temperatures (or, e.g., by using sinter aids or by using wide porous zirconia support materials) substantially improves the butadiene selectivity.

ACKNOWLEDGMENTS

L. B. thanks M. W. J. van Soest, W. J. Fok, S. Flink, B. B. Wentzel, and E. K. de Wit for experimental work and discussions.

REFERENCES

1. Boot, L. A., van Dillen, A. J., Geus, J. W., and van Buren, F. R., *J. Catal.* **162**, 1996.
2. Stobbe, D. E., Ph.D. thesis, Utrecht University, 1990.
3. Stobbe, D. E., van Buren, F. R., Stobbe-Kreemers, A. W., Schokker, J. J., van Dillen, A. J., and Geus, J. W., *J. Chem. Soc. Faraday Trans.* **87**, 1623 (1991).
4. Stobbe, D. E., van Buren, F. R., Hoogenraad, M. S., van Dillen, A. J., and Geus, J. W., *J. Chem. Soc. Faraday Trans.* **87**, 1639 (1991).
5. Stobbe, D. E., van Buren, F. R., van Dillen, A. J., and Geus, J. W., *J. Catal.* **135**, 533 (1992).
6. Stobbe, D. E., van Buren, F. R., van Dillen, A. J., and Geus, J. W., *J. Catal.* **135**, 548 (1992).
7. Boot, L. A., Ph.D. thesis, Utrecht University, 1994 (ISBN 90-393-0895-0).

8. Barin, I., and Knacke, O., "Thermochemical Properties of Inorganic Substances." Springer, Berlin, 1973.
9. Barin, I., Knacke, O., and Kubaschewski, O., "Thermochemical Properties of Inorganic Substances (Supplement)." Springer, Berlin, 1977.
10. Lee, E. H., *Catal. Rev.* **8**, 285 (1973).
11. Dadyburjor, D. B., Liu, Z., Matoba, S., Osanai, S., and Shiro-oka, T., *in* "Studies in Surface Science and Catalysis" (B. Delmon and G. Froment, Eds.), Vol. 88, p. 273. Elsevier, Amsterdam, 1994.
12. Courty, Ph., and Le Page, J. F., *in* "Studies in Surface Science and Catalysis" (B. Delmon, P. Grange, P. Jacobs, and G. Poncelet, Eds.), Vol. 3, p. 293, Elsevier, Amsterdam, 1979.
13. Satterfield, C. R., "Mass Transfer in Heterogeneous Catalysis." MIT Press, Cambridge, MA, 1970.
14. Boot, L. A., van der Linde, S. C., van Dillen, A. J., Geus, J. W., van Buren, F. R., and Bongaarts, J. E., *in* "Studies in Surface Science and Catalysis" (B. Delmon and G. Froment, Eds.), Vol. 88, p. 491. Elsevier, Amsterdam, 1994.